Fluorescent and Photoactivatable Fluorescent Derivatives of Tetrodotoxin To Probe the Sodium Channel of Excitable Membranes†

Kimon J. Angelides*

ABSTRACT: Fluorescent and photoactivatable fluorescent derivatives of tetrodotoxin (TTX) have been synthesized. *N*-Methylanthraniloylglycine hydrazide, anthraniloyl hydrazide, and 2-azidoanthraniloylglycine hydrazide were coupled to the carbonyl at C_6 of oxidized tetrodotoxin to form stable fluorescent hydrazones. The C_6 ketone can be reductively aminated with either ammonium or methylammonium acetate to form 6-amino- or 6-(methylamino)tetrodotoxin, which can then be acylated by a variety of fluorescent reagents. The biological activity, competitive binding with [^{3}H]tetrodotoxin for the receptor on rat axonal membranes, and equilibrium binding isotherms obtained by fluorescence enhancement or anisotropy indicate that the derivatives are only about 2–5 times less active than tetrodotoxin itself. The 2-azidoanthraniloylglycine hydrazone of oxidized tetrodotoxin, when activated by light, generates a reactive nitrene which is capable of covalent insertion into the toxin receptor. The product of the photolysis is a highly fluorescent tetrodotoxin derivative which is irreversibly linked to the receptor site. The excitation and emission spectra of the fluorescent tetrodotoxin derivatives vary with solvent polarity, and this sensitivity has been used to determine the immediate environmental characteristics of the toxin binding site of the sodium channel. It is concluded that the toxin binding site is highly polar. Emission and excitation spectra reveal that radiationless energy is transferred from tryptophan residues of the receptor to the anthraniloyl group of the TTX derivatives.

Propagation of the action potential of nerve cells is generally thought to occur by transient changes in the permeability of the cell membrane to Na^+ ions via a specific channel. Two major events can be distinguished in the passage of Na^+ through the channel: (1) selective filtering for Na^+ ions and (2) increases in the permeability to Na^+ by many orders of magnitude by a type of gating mechanism with kinetics sufficient for opening and closing.

The pufferfish toxin, tetrodotoxin (TTX),[1] has been very useful for identifying Na^+ channel since it selectively eliminates the transient current while not affecting the functioning of the gating system. Presumably its mode of action is through a very selective and tight association with the selectivity filter of the Na^+ channel, the charged guanidinium group mimicking the hydrated Na^+ ion, and the hydrophilic portions of the molecule forming hydrogen bonds with the channel binding site (Hille, 1975a). The availability of radiolabeled tetrodotoxin has permitted thermodynamic and kinetic studies of the channel–toxin interaction in a number of excitable membranes (Henderson & Wang, 1972; Balerna et al., 1975; Armstrong, 1975; Reed & Raftery, 1976; Ritchie & Rogart, 1977) as well as first experiments aimed at the solubilization and purification of the toxin binding component (Benzer & Raftery, 1972; Agnew et al., 1978; Agnew & Raftery, 1979). However, there are relatively few reports on the molecular characteristics of the ion channel in the intact nerve cell.

In view of the high specificity of tetrodotoxin for inhibition of the Na^+ channel, we have prepared fluorescent and photoactivated fluorescent derivatives of tetrodotoxin to be used as active site directed probes for this particular membrane component. The irreversibility of the photoactivated product can be used to facilitate the isolation and chemical characterization of the ion channel while the fluorescent properties can be used to determine the locations of the functional sites of the channel, to describe the conformational states and microenvironment of the toxin site, and to facilitate microscopic visualization of the channel in the membrane of selected nerve cells. In this study, tetrodotoxin has been modified to prepare derivatives which bind tightly to the toxin site on axonal membranes. The binding, spectroscopic characterization, and the effect of other ligands on the fluorescence of these TTX derivatives are presented.

Experimental Procedures

Materials. The hydrazine hydrate (85%), sodium nitrite, sodium cyanoborohydride, periodic acid, glycine ethyl ester hydrochloride, quinine bisulfate, 2,4-dinitrophenylhydrazine, and triethylamine were from Aldrich. Citrate-free tetrodotoxin was from Calbiochem, was tritiated at ICN by the Wilzbach method, and was purified as described (Benzer & Raftery, 1972) to a specific activity of 0.38 Ci/mmol. [^{14}C]Glycine ethyl ester hydrochloride (specific activity 46.9 mCi/mmol), sodium [^{3}H]borohydride (specific activity 18.3 Ci/mmol), and [^{14}C]methylamine (specific activity 48.1 mCi/mmol) were from New England Nuclear. *N*-Methylisatoic anhydride, isatoic anhydride, anthranilic acid, anthraniloyl hydrazide, pyrenebutyryl hydrazide, and NBD-Cl were from Molecular Probes, Inc. Other chemicals were the best available commercial grades, and deionized distilled water was used in all solutions.

† From the Department of Biochemistry, McGill University, Montreal, Quebec, Canada H3G 1Y6. *Received June 25, 1980; revised manuscript received February 9, 1981.* This work was supported by grants from The Research Corporation and The Medical Research Council of Canada.

* Correspondence should be addressed to this author at the Department of Biochemistry and Molecular Biology, University of Florida, Gainesville, FL 32610.

[1] Abbreviations used: TTX, tetrodotoxin; AAG, 2-azidoanthraniloylglycine; NMAG, *N*-methylanthraniloylglycine; ANT, anthraniloyl; AAG-TTX, 2-azidoanthraniloylglycine hydrazone of oxidized TTX; NMAG-TTX, *N*-methylanthraniloylglycine hydrazone of oxidized TTX; ANT-TTX, anthraniloylhydrazone of oxidized TTX; 2,4-DNPH, 2,4-dinitrophenylhydrazine; Me_2SO, dimethyl sulfoxide; $NaCNBH_3$, sodium cyanoborohydride; NH_2-TTX, 6-aminotetrodotoxin; CH_3-NH-TTX, 6-(methylamino)tetrodotoxin; NBD-Cl, 7-chloro-4-nitro-2,1,3-benzoxadiazole; Hepes, *N*-(2-hydroxyethyl)piperazine-*N*′-2-ethanesulfonic acid; Tris, tris(hydroxymethyl)aminomethane.

0006-2960/81/0420-4107$01.25/0

Analytical and preparative thin-layer chromatography was performed on Eastman cellulose-coated plates (0.16 mm), Macherey-Nayel (Düren, West Germany) silica gel G plates (0.1 mm), and Analtech silica gel G (0.25 mm). Sephadex LH-20 was from Pharmacia Fine Chemicals.

Methods. Axolemma membrane vesicles from rat brain white matter were prepared according to the method of De Vries et al. (1978). The 1.0/1.2 fraction was used since the myelin contamination in the fraction was minimal (0.035% of the total protein), determined by radioimmunometric assay for myelin basic protein (Cohen et al., 1975). Protein content was determined by the method of Bradford (1976).

Oxidation of TTX at carbons 6 and 11 was performed essentially as described by Chicheportiche et al. (1979). Citrate-free TTX (2.0 mg, 6.28 μmol) was dissolved in 0.2 mL of distilled water with 2.0 μL of trifluoroacetic acid added (pH in test solutions 2.3). The solutions was lyophilized and redissolved in 0.2 mL of distilled water (pH final in test solutions 5.5) in a polyethylene Eppendorf minifuge tube. Periodic acid (6.3 μmol) was added, and the reaction mixture was allowed to react at 25 °C for 30 min. Lead(II) acetate (6.4 μmol) was added to the reaction mixture at 4 °C to precipitate excess iodide ions, and the precipitate of lead diiodide was removed by centrifugation in an Eppendorf minifuge. The supernatant was carefully removed and lyophilized. The oxidized product could be identified on a silica gel G plate by spraying with a 0.5% solution of 2,4-DNPH in 1 N HCl or pyrenebutyryl hydrazide in methanol: R_f (chloroform–methanol, 2:1 v/v) 0.08. In addition, migration of TTX could be followed by spraying with alcoholic KOH and heating (Mosher et al., 1964): R_f (ethanol–acetic acid, 96:4 v/v) 0.38.

The preparation of 6-amino-TTX and 6-(methylamino)-TTX followed the pattern detailed by Varlet et al. (1978) for 2-aminoalkanephosphoric acids. The reactions were performed by dissolving a mixture of oxidized TTX (6.0 μmol), NH_4OAc or methylammonium acetate (32 μmol) with [^{14}C]methylammonium acetate as tracer, and 4.2 μmol of $NaCNBH_3$ in 3.0 mL of absolute methanol in a screw-capped conical vial. The kinetics of the reaction were followed by removing aliquots of the reaction mixture (10 μL) at selected times and reacted with 2–5 μL of fluorescamine (0.4 mg mL^{-1} in acetonitrile). Excitation was at 390 nm and emission at 480 nm. Fluorescence controls were done in which the oxidized TTX was omitted from the reaction mixture. In these instances, a very small amount (<8%) of fluorescamine fluorescence was observed. The reaction was complete after 48 h when no further increase in the fluorescamine fluorescence appeared.

Syntheses of Fluorescent TTX Derivatives. All synthetic work was done in a darkroom under red light or in dim room light.

(*A*) *2-Azidoanthraniloylglycine Hydrazide* (*AAG*). Isatoic anhydride (326 mg, 2 mmol) was added to 349 mg (2.5 mmol) of glycine ethyl ester (containing a small amount of [^{14}C]-glycine ethyl ester) in 30 mL of 30% water–70% dioxane. After addition of 7.5 mmol of triethylamine (1.05 mL) (freshly distilled), the reaction was stirred and the temperature slowly raised until a moderate evolution of CO_2 gas occurred. This was around 70 °C. After the isatoic anhydride was consumed and gas evolution had ceased, the mixture was cooled, and solid started to precipitate almost immediately. The mixture was allowed to stand in the refrigerator overnight, and the amide was isolated by acid–base and ether extraction (Staiger & Miller, 1959). The product was recrystallized from methanol–water: yield, 68% (304 mg). The radiolabeled derivative using [^{14}C]glycine ethyl ester was purified by preparative thin-layer chromatography on silica gel G with chloroform/methanol (3:1) solvent: R_f 0.92; NMR δ 6.65 (Ph H-3), 7.17 (Ph H-4), 9.56 (Ph-2NH_2), 6.71 [C(=O)NH], 3.97 (NC-H_2CO), 4.18 (OCH_2), and 1.26 (CH_3 ester).

Transformation of the 2-amino group to an azido function was performed by dissolving 178 mg of anthraniloylglycine ethyl ester (0.8 mmol) in 0.5 N HCl with 30% ethanol. Sodium nitrite (58 mg, 0.8 mmol) in 1.0 mL of cold water was added, and the reaction mixture was stirred at 4 °C for 90 min. The excess nitrous acid was then expelled by degassing. Sodium azide (52 mg, 0.8 mmol) in 1 mL of cold water was slowly added to the stirring solution at 4 °C and left to react for 45 min, after which time the material precipitated. The material was filtered and dried over P_2O_5 overnight in the dark. Infrared spectroscopy in KBr disks verified the presence of the azido group (N_3, 2120 cm^{-1}). Hydrazine hydrate (0.56 mL in 6.5 mL of absolute ethanol) was added to 158 mg (0.64 mmol) of 2-azidoanthraniloylglycine ethyl ester in 20 mL of absolute ethanol. The mixture was refluxed for 60 min, after which time the solvent was removed by rotoevaporation. Thin-layer chromatography (chloroform/methanol, 3:1) on cellulose indicated complete disappearance of the ester and formation of a new, slower moving product. Recrystallization from ethanol–water gave 112 mg of pure product (87% yield): R_f 0.58 in acetone. Proton NMR (Me_2SO-d_6) showed disappearance of the ester resonances and appearance of δ 3.9 (br s, 3 H, NH).

(*B*) *N-Methylanthraniloylglycine Hydrazide* (*NMAG*). *N*-Methylisatoic anhydride (300 mg, 2.9 mmol) was dissolved in 5 mL of Me_2SO followed by 404 mg of glycine ethyl ester (2.9 mmol) dissolved in 10 mL of Me_2SO and 3 equiv of triethylamine. The reaction mixture was heated to 60 °C until all gas evolution ceased. The solvent was removed in vacuo onto Celite. Recrystallization from ethanol–water gave pale yellow crystals which chromatographed in chloroform/methanol (3:1) and had bright blue fluorescence: NMR (Me_2SO-d_6) δ 3.29 (Ph-N-CH_3). Other resonances were similar to AAG. Conversion to the hydrazide derivative was done as described above for 2-azidoanthraniloylglycine ethyl ester.

Recrystallization from absolute ethanol gave 437 mg (67%) of pure product: R_f (chloroform/methanol, 3:1) 0.08 and (acetone adduct) 0.68; proton NMR δ 3.9 [br, C(=O)-$NHNH_2$].

Coupling of Hydrazide Derivatives to Oxidized TTX. All coupling reactions were performed in a 1-mL screw-capped conical vial with a silicone membrane, and the manipulations were done with a syringe through the membrane. Oxidized TTX (1 mg, 3.14 μmol) was dissolved in 300 μL of acidified methanol (pH_{app} 5.3), and 9.6 μmol of fluorescent hydrazide derivative was added. The reaction was carried out over molecular sieves (3 Å) to remove the water which is eliminated during the course of the coupling reaction. The reaction was allowed to proceed at 37 °C, and the kinetics were followed by thin-layer chromatography in acetonitrile/0.1 M ammonium formate (pH_{app} 5.2). After 5 h, all the insoluble material solubilized, and the kinetics of the reaction indicated that equilibrium had been reached. Alternatively, 1 mg of oxidized TTX was dissolved in 300 μL of water acidified with 1 μL of trifluoroacetic acid, lyophilized, and then redissolved in 200 μL of anhydrous Me_2SO. Dimethyl sulfoxide was then used as the solvent for the coupling reaction and could be removed by lyophilization. Reduction by $NaCNBH_3$ was performed by adding 5.0 μmol of $NaCNBH_3$ in absolute methanol to the coupled fluorescent TTX in 300 μL of methanol (pH_{app} 6.8), and reduction was allowed to proceed for 52 h at 37 °C. The

reaction mixture was redissolved in a minimum (200 μL) of acidified methanol (pH_{app} 5.3) and applied to a Sephadex LH-20 column preequilibrated with acidified methanol. The column was eluted with acidified methanol (pH_{app} 5.3) and a linear salt gradient consisting of 0.01–0.15 M ammonium formate (pH final 5.5). Fractions of 200 μL were collected. The fractions were then subjected to analysis for unreacted tetrodotoxin by the fluorescence method under alkaline conditions (excitation 390 nm, emission 500 nm) (Nũnez et al., 1976) and for the product formation (excitation 325 or 350 nm, emission 405 or 425 nm) as well as for determination of radioactivity when [^{14}C]glycine ethyl ester was used as reagent. The fractions which showed evidence for coupled tetrodotoxin product were then analyzed and repurified by two-dimensional thin-layer chromatography on silica gel G plates with chloroform/methanol (3:1) in the first dimension followed by acetonitrile/0.1 M ammonium formate (pH_{app} 5.2) in the second (Chicheportiche et al., 1979). The product remained at the origin in the first dimension while the uncoupled hydrazides migrated with an R_f of ~0.85. In the second dimension, the following R_f values were determined: AAG-TTX, 0.33; NMAG-TTX, 0.63; ANT-TTX, 0.46.

Binding Measurements. The binding of [^{3}H]TTX to axolemma vesicles was studied by the technique of forced dialysis at 25 °C (Cantley & Hammes, 1973). XM-50 ultrafiltration membranes (Amicon) were used to exclude all protein. Because these membranes must be used damp, approximately a 5-μL dilution of the ligand occurs in the first sample forced through the membrane. Therefore, five 30-μL aliquots were collected, and the last three were used to determine the free ligand concentration. Samples were counted for radioactivity in Aquasol II on an Intertechnique scintillation counter. Counting efficiency was determined by the method of internal standards. Fluorescence titrations of the binding of NMAG-TTX to axolemma were done at three different membrane protein concentrations. Inner filter effects of anthraniloyl absorbance were negligible as the concentration of the ligand was always less than 10 μM in the solution on which fluorescence measurements were made. With the optical settings held constant through a given set of measurements, the fluorescence intensity was linear with ligand concentration, as verified by test solutions. In order to measure the amount of [^{3}H]TTX or fluorescent TTX specifically bound at the toxin binding site, 2–10 μM of TTX was preequilibrated with membranes, and the binding measurements with [^{3}H]TTX or fluorescent compounds were repeated under these conditions. In this manner, the amount of nonspecific binding was determined, and the data were corrected accordingly. Unless otherwise noted, the buffer used was composed of 10 mM Hepes adjusted to pH 7.4 with Tris-HCl, 160 mM NaCl, 5.4 mM KCl, 5 mM $MgSO_4$, and 2 mM $CaSO_4$.

Spectroscopic Measurements. Ultraviolet–visible spectra were determined with a Cary 14 spectrophotometer and infrared spectroscopy with a Perkin-Elmer 257 spectrophotometer. Proton NMR spectra were taken on a Varian XL-200 Fourier transform (200-MHz) spectrometer. A minimum of 20 000 transients were accumulated for each TTX spectrum. All fluorescence measurements were made with a SLM 4800 subnanosecond spectrofluorometer interfaced to a PDP/MINC 11 computer (Digital Equipment Corporation). Measurements were made in 0.3 × 0.3 cm fluorescence microcuvettes with a capacity of 150 μL to minimize inner filter effects. Shutters were closed between measurements. The fluorescence measurements were made with the sample holder thermostated at 25 °C. Fluorescence spectra were corrected for wavelength-dependent variation in light source output, phototube response, and monochromator efficiency.

In titrations of the fluorescence of binding to the membrane, several control experiments were performed. For example, to measure the fluorescence enhancement of fluorescent TTX derivatives upon binding to axonal membranes, parallel experiments using identical solutions and instrument settings were performed but in the absence of membranes. The fluorescence vs. concentration plot was linear through the concentration range studied. In the figure presented, ΔF is the difference in fluorescence intensity of the fluorophore in the presence of membranes and that in the absence of membranes. All titrations were also corrected for dilution effects. Corrected emission spectra were computed by comparison with the spectrum of quinine bisulfate in 0.1 N H_2SO_4 with excitation at the appropriate wavelength at 25 °C (Velapoldi & Mielenz, 1980). A comparative method (Parker & Rees, 1966) was used to determine the quantum yields of NMAG-TTX and ANT-TTX bound to axonal membranes. Equation

$$Q_1/Q_2 = (F_1/F_2)(A_2/A_1)/(1 - r_b/4) \quad (1)$$

1 gives the ratio of quantum yields, Q_i, as a function of the area of the corrected emission spectrum, F_i, and the absorbance at the exciting wavelength, A_i, for two different fluorophores. The factor $1 - r_b/4$ is a correction for polarized emission (Shinitzky, 1972), and r_b is the anisotropy of the fluorophore. Both A_1 and A_2 were kept below 0.05A to minimize inner filter effects. An absolute quantum yield of 0.7 was used for quinine sulfate in 0.1 N H_2SO_4 at 23 °C with an exciting wavelength of 350 nm (Scott et al., 1970). The magnitude of light scattering by membranes was determined by measuring the apparent fluorescence emission spectrum starting at 360 nm with excitation at 345 nm, where no significant *N*-methylanthraniloyl fluorescence occurs.

Fluorescence anisotropies were measured by using the T format of the spectrofluorometer which simultaneously measures the ratio of the vertical and horizontal components of emitted light with the exciting light either vertically polarized $(V/H)_v$ or horizontally polarized $(V/H)_h$. The anisotropy is defined by eq 2 where $(V/H)_h$ corrects for unequal trans-

$$r = \frac{(V/H)_v - (V/H)_h}{(V/H)_v + 2(V/H)_h} \quad (2)$$

mission of horizontally and vertically polarized light (Azumi & McGlynn, 1962). The limiting fluorescence emission anisotropy was determined by extrapolating the linear portion of a Perrin plot ($1/r$ vs. T/η) to infinite viscosity as described by Dale & Eisinger (1975). The viscosity was varied by increasing the sucrose concentration at constant temperature.

Since the anthraniloyl derivatives fluoresce in solution as well as when bound to the receptor, the quantum yield of the bound fluorophore was computed from the measured overall quantum yield by using the relationship

$$Q_{obsd} = x_f Q_f + x_b Q_b \quad (3)$$

where x_f and x_b are the mole fractions of free and bound fluorescent toxins and the Q's are the corresponding quantum yields. The quantum yield of the free fluorescent TTX was measured in a solution without axonal membranes; in the presence of membranes, the concentration of the bound fluorescent TTX was calculated by assuming a dissociation constant of 7.1 nM for NMAG-TTX and 6.1 nM for ANT-TTX and assuming the absorbance spectra of these derivatives do not change when bound to the membrane receptor. In some cases with low light levels, the monochrometers were removed, and Schott KV filters were used to isolate the desired wave-

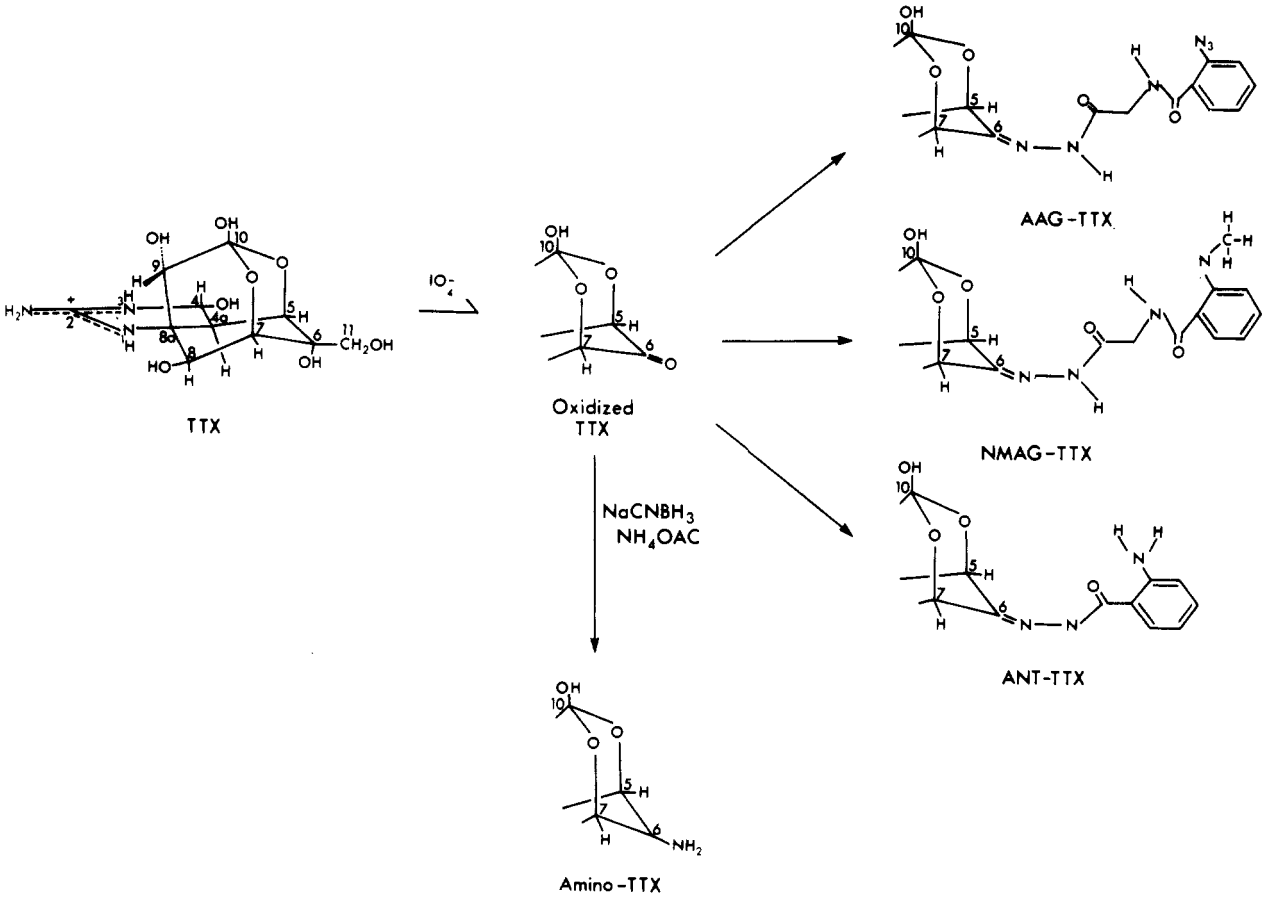

FIGURE 1: Structure of TTX and derivatives of TTX.

length of excitation or emission. Light scattering was measured under the same conditions but in the absence of the fluorescent label.

Electrophysiological Measurements. Frog sciatic nerves, dissected and desheathed, were placed in a chamber with five compartments according to Strong et al. (1973), except that the capacity of the center test pool containing the sample of TTX or TTX derivatives to be assayed was 200 μL. The biphasic compound action potential was amplified and displayed on an oscilloscope. Compound action potentials of over 60 mV were generally recorded. The activity of TTX and TTX derivatives was assessed by the ability of the toxin to decrease the amplitude of the rising phase of the action potential. Appropriate controls were performed by use of Ringer's solution with no toxin added.

Photolysis. Photoirradiation was performed by using the 450-W xenon lamp of the spectrofluorometer with the sample thermostated at 25 °C. The excitation slits in these experiments were set at 16 nm at the desired wavelength of irradiation and the emission slits at 4 nm. The corresponding time-dependent changes in the fluoroescence intensity were followed by using the time base mode of the spectrofluorometer.

Results

Preparation of Fluorescent TTX Derivatives. The structures of TTX, oxidized TTX, amino-TTX, AAG-TTX, NMAG-TTX, and ANT-TTX are shown in Figure 1. Most attempts to modify TTX have led to derivatives which are either biologically inactive or retain only partial biological activity (Narahashi et al., 1967; Strong & Keana, 1976). Recently, however, oxidation of the vicinal hydroxyls at C_6 and C_{11} leading to a biologically active toxin has been accomplished and has permitted the preparation of a variety of TTX derivatives (Tsien et al., 1975; Chicheportiche et al., 1979, 1980). The secondary and primary alcohols at C_6 and C_{11} were utilized in this work to prepare a ketone at C_6 which can be subsequently condensed to fluorescent and photoactivatable fluorescent hydrazides. Conversion to the ketone was verified by reacting the product with 2,4-dinitrophenylhydrazine or pyrenebutyryl hydrazide to give the corresponding hydrazones. Oxidation at C_6 and C_{11} positions was also confirmed by 200-MHz proton NMR spectroscopy in which the C_{11} proton resonances [(*tert*-butyl alcohol) δ 4.018 and 4.019 (d, J = 0.19 Hz)] were essentially eliminated. Retention of structure at positions 4a and 4 after periodiate oxidation was established by the retention of the two doublets and the coupling constants of the 4a-H [δ 2.323 and 2.371 (J = 9.47 Hz)] and 4-H protons [δ 5.463 and 5.511 (J = 9.52 Hz)]. The protons ascribed to the 4a doublet position, however, showed a slight downfield shift to 2.194 and 2.241 ppm (J = 9.46 Hz) and the 4 position, 5.508 and 5.461 ppm (J = 9.33 Hz). A more detailed analysis of these spectra will be presented (N. W. Ross and K. J. Angelides, unpublished results). The extent of tetrodotoxin oxidation, assessed to be 92%, was quantitated either spectrophotometrically or fluorometrically by using the absorbance at 362 nm (ϵ = 27940 M^{-1} cm^{-1}) for 2,4-DNPH or 342 nm for pyrenebutyryl hydrazide (ϵ_{342} = 38000 M^{-1} cm^{-1}; Holowka & Hammes, 1977) and emission at 379 nm. Pyrenebutyryl hydrazide, in particular, provides a very sensitive marker for small amounts due to its high extinction coefficient and efficient quantum yield (~0.3). The main difficulties in preparing TTX derivatives generally result from (1) the necessity of working with minute quantities of the toxin, (2) the low solubility of TTX in most organic solvents needed to carry out the modification reactions, (3) the sensitivity to modification at other centers on the native molecule, and (4) separation of unmodified toxin from the derivatized toxin.

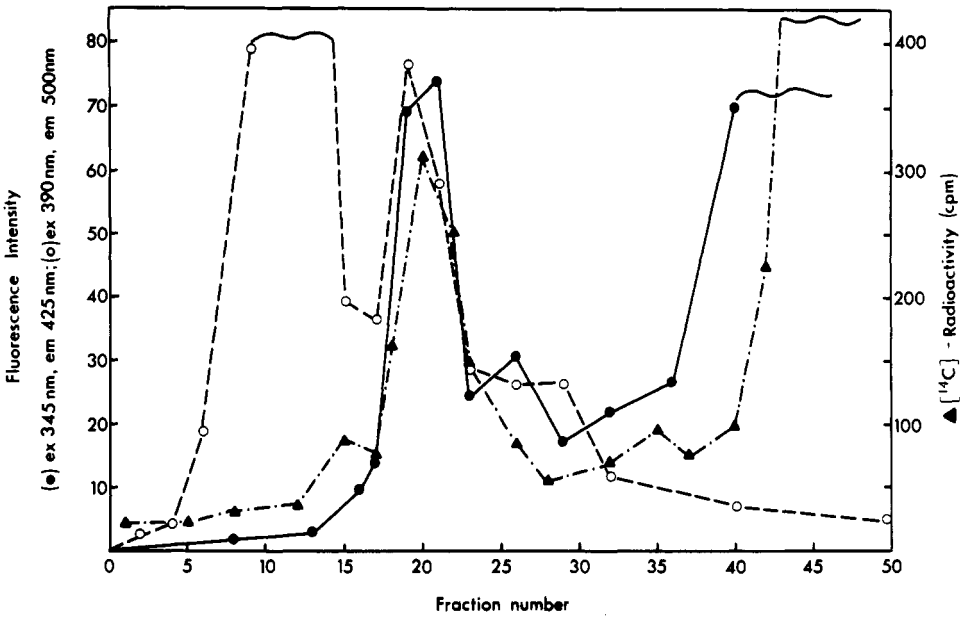

FIGURE 2: Purification of NMAG-TTX by chromatography on Sephadex LH-20. A 200-μL volume of reaction product was applied to a column of LH-20 (1.5 × 7 cm) and eluted with acidified methanol (pH_{app} 5.3) and a salt gradient from 0.01 to 0.15 ammonium formate (pH final 5.5); 200 μL fractions were collected. Excitation at 345 nm and emission at 425 nm represent the fluorescent hydrazide (●), excitation at 390 nm and emission at 500 nm represent alkali-treated tetrodotoxin (○), and radioactivity represents the glycine moiety (▲). Fractions 16–30 were collected and further purified by two-dimensional chromatography on silica gel G.

Oxidized TTX can be effectively solubilized in acidified methanol or Me_2SO after one lyophilization–solubilization cycle, which thereby increases the effective concentration of the reactant. The coupling reaction of oxidized TTX with the fluorescent hydrazides involves the formation of a hydrazone by elimination of the elements of water which, in principle, can be stabilized by reduction with borohydrides. By carrying out the reaction in the presence of molecular sieves, the yield of the hydrazones has been significantly improved since the water formed is rapidly removed and hydrolysis of the hydrazone is considerably reduced. Only in the case of NMAG-TTX, however, has the hydrazone produced been reducible with $NaCNBH_3$ at pH 6.5, where this reagent is sufficiently stable as compared with sodium borohydride, to yield a biologically active derivative. Reduction by [^{3}H]NaBH_4 at pH 9 (where the stability of $NaBH_4$ necessitates the high pH) led to a biologically inactive product. The extent of reduction is not known, although incorporation of tritium indicates that reduction is about 83% complete. The final yield of coupled product is 18%. The increase in stability and yield (18%), compared to 5–10% (Chicheportiche et al., 1979), in this study reflects in part the solubilization of oxidized TTX, the removal of water during the course of the coupling reaction, and the stabilization of the hydrazone by reduction with sodium cyanoborohydride.

Separation of unmodified toxin and purification of fluorescent derivatives are crucial steps in the preparation of TTX derivatives since minute amounts of unmodified toxin can mask the biological effects of the modified toxin. A typical purification of NMAG-TTX by Sephadex LH-20 in the presence of a linear salt gradient is given in Figure 2. The eluate was followed by ^{14}C radioactivity (contained in the glycine moiety), the fluorescence (excitation 345 nm, emission 425 nm) of the *N*-methylanthraniloyl group, and the fluorescence of alkali-treated fractions (excitation 390 nm, emission 500 nm) for the tetrodotoxin moiety of the fractions. Separation of unreacted oxidized TTX, NMAG-TTX, and unreacted fluorescent hydrazide was satisfactorily accomplished by using Sephadex LH-20 with methanol as the eluting solvent. The *N*-methylanthraniloylglycine-coupled TTX is retarded due to absorption of the aromatic group to the column while unreacted TTX eluted in the first fractions. The unreacted fluorescent anthraniloyl hydrazides eluted in the last fractions due to their greater absorption of the column. A linear salt gradient facilitated elution of the TTX fractions since it was initially observed that TTX itself is slightly retained by the Sephadex LH-20 column, probably due to hydrogen bonding between the glucose hydroxyls of the resin and the functional groups of TTX. This purification procedure results in a satisfactory separation of fluorescent TTX derivatives from the excess of fluorescent hydrazides and from unreacted oxidized TTX. Further purification of the labeled TTX was achieved by two-dimensional thin-layer chromatography on silica gel G using the solvent systems described by Chicheportiche et al. (1979), followed in some cases by preparative paper electrophoresis at 40 V/cm in pyridine/acetic acid/water (25:1:225) at pH 6.5 (Ross & Angelides, 1980; N. W. Ross and K. J. Angelides, unpublished results). NH_2-TTX and CH_3-NH-TTX (net charge +2 at pH 6.5), in particular, could be easily separated by this method since they electrophorese nearly twice as far from the origin toward the cathode than unmodified TTX or oxidized TTX. Either NH_2-TTX or CH_3-NH-TTX can be identified by spraying with a solution of 0.2% fluorescamine in methanol or 0.5% NBD-Cl in ethanol, respectively. When the fluorescent derivatives are kept at −70 °C at high concentrations, under anhydrous conditions, e.g., 5.0 mM, their stability and biological activity are quite good (5% decomposition a month).

The stoichiometry between TTX and the fluorescent component was determined by the ratio of fluorescence intensities as measured above for each moiety. The extinction coefficients or fluorescence properties of the anthraniloyl compounds are not altered when coupled to TTX (see below). In this manner, 0.82 ± 0.16 mol of ANT per mol of TTX, 0.92 ± 0.10 mol of NMAG per mol of TTX, and 0.94 ± 0.08 mol of AAG per mol of TTX were found.

Biological Activity. Figure 3 shows the effect of TTX, NMAG-TTX, ANT-TTX, and AAG-TTX on frog sciatic nerve potentials. A detailed comparison of the action of TTX and fluorescent TTX derivatives is illustrated in Figure 3A

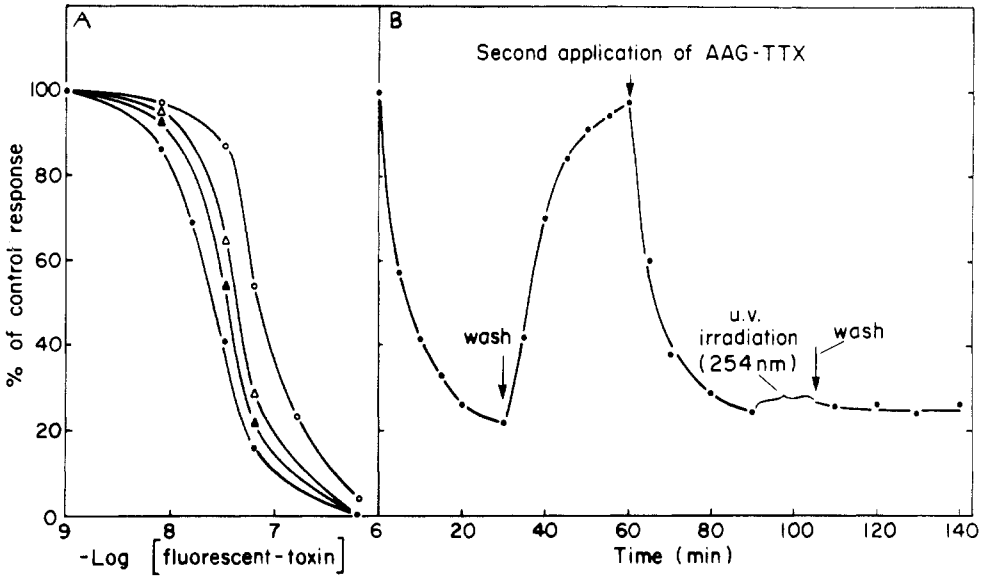

FIGURE 3: Effect of TTX and fluorescent TTX derivatives on frog sciatic nerve potentials. Experiments were carried out at 37 °C in Ringer's solution, pH 7.3, in a final volume of 200 μL. The toxins were diluted into the experimental buffer, and the potential measurements were recorded at various times until equilibrium was reached. Stimulation was at 0.5 or 1.0 Hz. (A) TTX (●), ANT-TTX (▲), NMAG-TTX (△), and AAG-TTX (○) antagonism of the nerve potential. The peak of the action potential is plotted as a function of increasing toxin concentration and expressed as the percentage decrease relative to a control to which no toxin was added. (B) Effects of 159 nm AAG-TTX on frog sciatic nerve potentials. The nerve preparation was perfused with 159 nM AAG-TTX under red light and washed with Ringer's solution, and a second aliquot of 159 nM AAG-TTX was applied. UV irradiation of AAG-TTX at 254 nm for 15 min by a Mineralight UVS-12 lamp induced irreversible association of AAG-TTX to the TTX receptor since extensive washing for 30–90 min did not restore the full control potential. Irradiation of the nerve at 254 nm for 15 min under these experimental conditions without AAG-TTX showed less than 10% loss in the full action potential.

Table I: Binding Parameters of Fluorescent TTX Derivatives

ligand	K_d (nM)	maximal binding capacity (pmol/mg of protein)	method	source
[^{3}H]TTX	3.2	3.8	direct binding forced dialysis	Figure 4A
NMAG-TTX	7.1	3.6	competitive binding	Figure 4B
	8.0	3.7	fluorescence enhancement	Figure 6
	6.8	3.4	energy transfer from Trp on axolemma membranes	Figure 6
	8.3	4.0	fluorescence anisotropy	Figure 7
ANT-TTX	6.1	3.5	competitive binding	Figure 4B
	6.6	4.2	fluorescence enhancement	Figure 5C
	5.8	3.7	energy transfer from Trp on axolemma membranes	data not presented
	6.4	3.9	fluorescence anisotropy	data not presented
AAG-TTX	16.8	3.5	competitive binding	Figure 4B

where the percentage decrease in action potential amplitude after 30 min of exposure to toxin, relative to experiments in which only Ringer's solution was applied, has been plotted as a function of the toxin concentration. From these data, the EC_{50} is 25 nM for TTX, 38 nM for ANT-TTX, 41 nM for NMAG-TTX, and 66 nM for AAG-TTX. The action of TTX and TTX derivatives was fully reversible upon 30 min of washing with buffer. In the presence of AAG-TTX, however, irradiation with a Mineralight UVS-12 (4-W and 1.4 mW/cm^2) lamp for 15 min resulted in a loss at equilibrium of 75% of the action potential amplitude that persisted even after extensive washing (Figure 3B).

Equilibrium Binding of Fluorescent TTX Derivatives to Rat Axonal Membranes. For determination of whether the fluorescent derivatives bind to axonal membranes and complete for the same site on the membrane as [^{3}H]TTX, equilibrium binding experiments were performed. Figure 4A shows the specific binding of [^{3}H]TTX to membranes performed by the forced dialysis technique, and the inset shows a Scatchard plot of these binding data. Specific binding was determined after correcting total binding for the nonspecific component (that observed in the presence of 2 μM unlabeled TTX) which was usually 10–20% of the total observed binding. The linearity of the Scatchard plot indicates a single set of binding sites with a maximum concentration of sites of 3.8 pmol/mg of protein and a dissociation constant of 3.2 mM. Figure 4B illustrates the binding of 100 nM [^{3}H]TTX to axonal membranes in the presence of varying concentrations of fluorescent toxins. The concentrations of the fluorescent TTX reagents were determined spectroscopically due to the limited availabilities of these compounds. It is evident that each of the fluorescent analogues strongly competes with [^{3}H]TTX binding to the receptor site. Moreover, the apparent dissociation constant of these derivatives varies from only about 2 to 5 times higher than that of TTX with comparable capacities for the receptor site. Scatchard analysis of these data suggests a single type of binding site for the receptor for these membranes. In the dark, the azido derivative binds reversibly and with high affinity to the TTX binding sites in the axolemma preparation. The data from Figure 4B together with the binding parameters obtained by other methods (see below) are summarized in Table I.

Spectral Characterization of Fluorescent TTX Derivatives and Receptor Binding Site. One of the major aims of this work is to be able to utilize these labels to derive information on

Table II: Spectral Properties of Anthraniloyl and Anthraniloyl-TTX Derivatives

axolemma		water	ethanol	1-butanol	acetonitrile	dioxane
(A) Excitation Maxima (nm)						
NMAG-TTX	352	NMAG 350 (1.79)[a]	354 (1.36)	356 (1.22)	356 (1.2)	355 (1)
ANT-TTX	325	ANT 321	332	328	326	322
(B) Emission Maxima (nm)						
NMAG-TTX	439	NMAG 432 (1.82)	418 (1.41)	416 (1.28)	412 (1.22)	406 (1)
ANT-TTX	402	ANT 398 (1.74)	387 (1.36)	383 (1.27)	381 (1.2)	379 (1)
AAG-TTX + membranes		AAG				
AAG-TTX + membranes (photolyzed)	402	AAG-TTX + membranes photolyzed 402 (1.69)	404 (1.28)	396 (1.21)	393 (1.15)	386 (1)

[a] Relative fluorescence intensity to compound in dioxane.

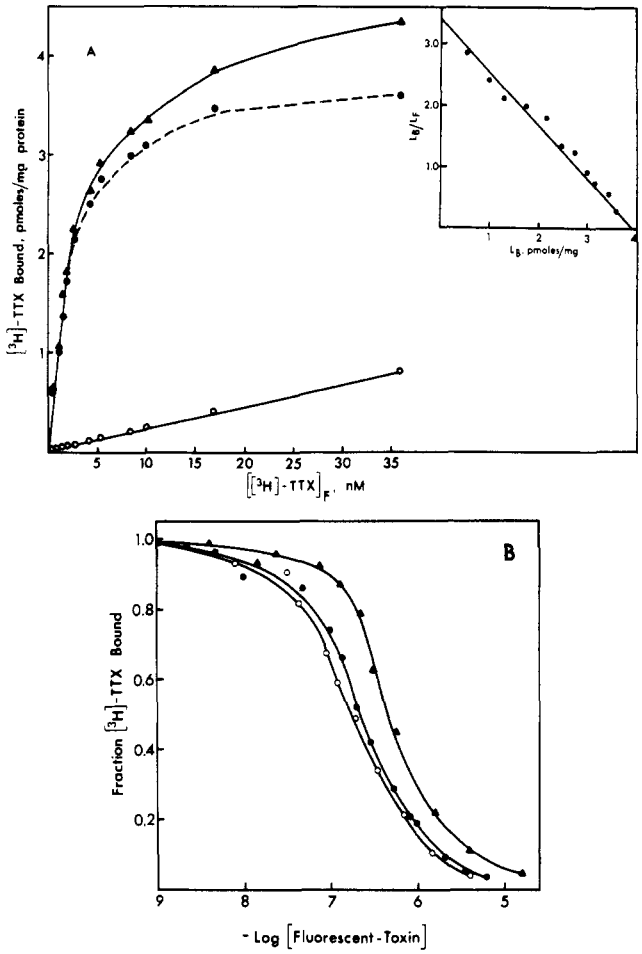

FIGURE 4: Binding of TTX and fluorescent TTX derivatives to rat axolemma. (A) Specific binding of [^{3}H]TTX to axolemma at 25 °C in the presence of 160 mM NaCl by forced dialysis. Specific binding (●) was determined as the difference between total [^{3}H]TTX binding (▲) and [^{3}H]TTX binding in the presence of 2 μM unlabeled TTX (○). (Inset) Scatchard plot of the specific binding. (B) Displacement of [^{3}H]TTX by fluorescent toxins. Axolemma were incubated at 25 °C for 30 min with 100 nM [^{3}H]TTX, and the indicated concentrations of ANT-TTX (○), NMAG-TTX (●), AAG-TTX (▲), and bound TTX were measured by forced dialysis. Nonspecific binding measured in the presence of 2 μM TTX has been subtracted from the results.

the molecular characteristics of the toxin receptor and to serve as site-specific probes in singlet–singlet energy transfer distance measurements between functional sites on the ion channel. Figure 5A shows the excitation spectra of NMAG-TTX and the fluorescence emission spectra of NMAG-TTX and ANT-TTX in the absence and in the presence of axonal membranes. Figure 5A shows that the excitation maxima are in the 320–360-nm range, as would be expected for anthraniloyl compounds.

Spectroscopic analysis of the uncoupled fluorescent hydrazide moieties, where sufficient quantities were available, allowed for determination of the extinction coefficients. Coupling to model compounds such as acetone, cyclohexanone, or α-ketononanoic acid showed no change in the absorption or fluorescent properties of the labels and was used to obtain fluorescence standard calibration–concentration curves. Because of the limited availability of labeled TTX, absorption or fluorometric measurements were used to determine the concentration of fluorescent TTX.

Excitation and emission spectra of NMAG, ANT, and AAG were obtained in solvents of varying polarity. The excitation and emission maxima are given in Table II. The emission maxima of these compounds are markedly dependent upon the polarity of the solvent. There is a shift of some 30 nm to the red as the solvent polarity increases from dioxane to water. In contrast, the solvent dependence of the excitation maxima is not appreciably affected. A significant shift to lower wavelengths is observed in going from dioxane to water. In fact, the excitation maxima in water are at lower wavelengths than in dioxane. In addition, as the solvent polarity increases, there is a broadening of the emission spectra, and the width of the emission spectrum at half-height for NMAG, for example, is 49, 54, 58, and 62 nm in dioxane, acetonitrile, ethanol, and water, respectively.

Fluorescence emission spectra of NMAG-TTX and ANT-TTX in the presence and absence of axonal membranes are shown in Figure 5B,C. It can be seen that the fluorescent compounds NMAG-TTX and ANT-TTX demonstrate considerable fluorescence enhancements upon addition of axonal membranes. Under these experimental conditions (46 nM sites), 85% of the NMAG-TTX and 87% of ANT-TTX are bound to the receptor. The observed quantum yields of the fluorescent toxins can be used in the expression given in eq 1 to calculate the quantum yields of the probe bound to the receptor. Comparison of the quantum yields of the anthraniloyl-TTX derivatives shows that the quantum yield of NMAG-TTX increases from 0.18 to 0.67 for the free and bound form and from 0.17 to 0.56 for the free and bound forms of ANT-TTX, in both cases an increase of approximately 4 times. When the bound toxins are displaced from the receptor by the addition of a 200-fold excess of TTX, the emission spectra return to the spectra of the free fluorescent toxins.

In addition, the fluorescence emission spectra exhibit a small red shift of ~7 nm. Spectra of the free fluorophores in these solvents suggest that the shift to lower energy in the fluorescence emission spectra are indicative of a more hydrophilic environment.

The fluorescent enhancement observed upon binding to axolemma vesicles can be utilized to determine the binding parameters of the fluorescent TTX derivatives to the receptor site. A fluorescence titration of axolemma membranes with

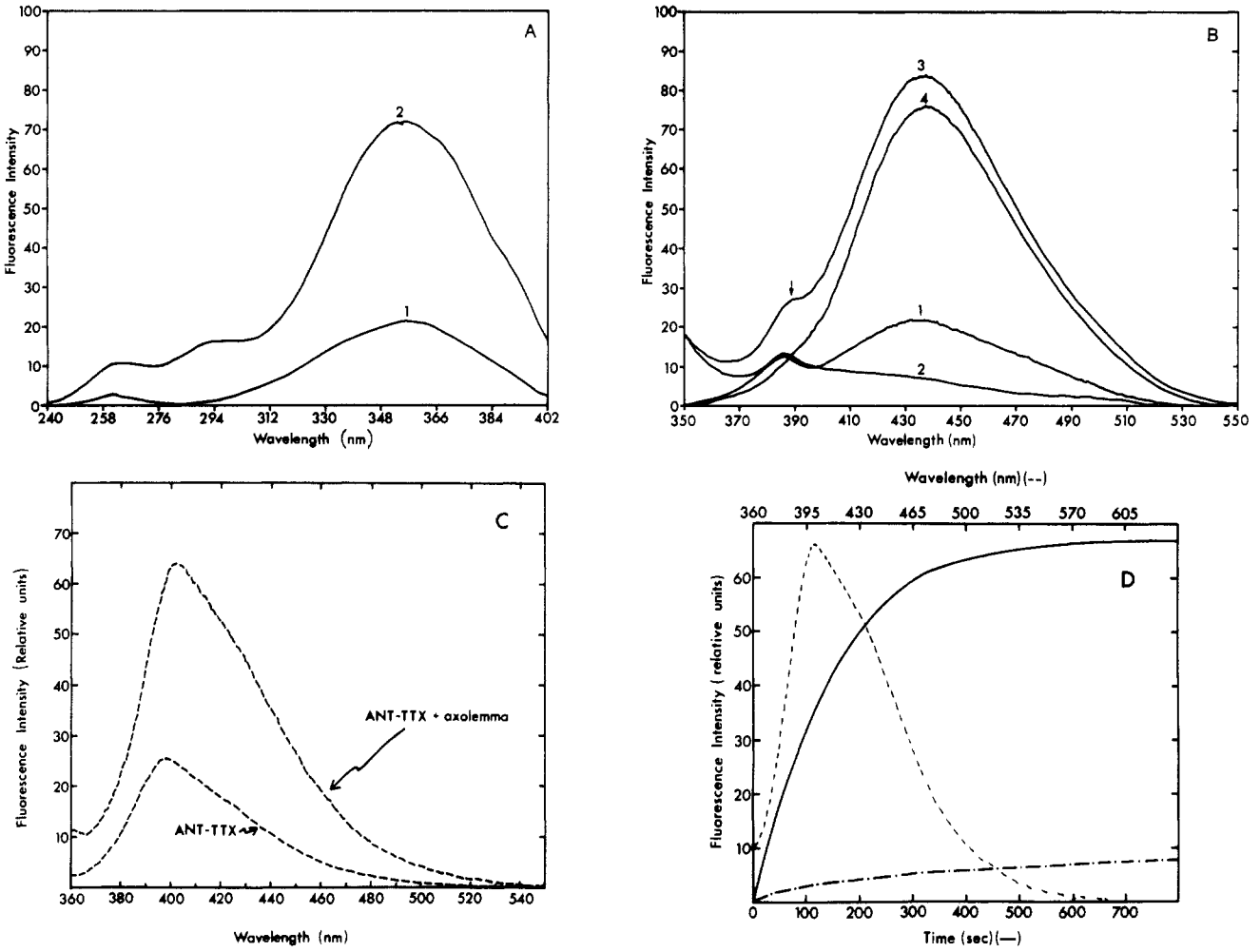

FIGURE 5: Excitation and corrected fluorescence emission spectra of ANT-TTX and NMAG-TTX free and bound to axonal membranes. The resultant spectra of the free fluorophore and fluorophore + axolemma represent difference spectra (five accumulations) of the fluorophore–solvent and fluorophore + membranes – membranes. The arrow indicates the position of solvent Raman bands. All measurements were in 0.3 × 0.3 cm microcuvettes to minimize inner filter absorption and light scattering. Axolemma concentration was 1.2 mg of protein. Identical instrument settings were used in the presence and absence of axolemma; however, the relative fluorescence intensities of the different probes may not be compared. (A) Excitation spectra of NMAG-TTX free (1) and bound to axonal membranes (2). Excitation resolution was 4 nm, and emitted light was isolated with a KV 418 filter. The spectra were recorded, and a blank of Hepes buffer or membranes was subtracted, as described above. Corrected fluorescence emission spectra of (B) NMAG-TTX ± axolemma (excitation at 345 nm). (1) 7.6 nM NMAG-TTX in Hepes buffer; (2) axonal membranes; (3) 7.6 nM NMAG-TTX + axolemma; (4) 7.6 nM NMAG-TTX + axolemma – axolemma. (C) ANT-TTX ± axolemma (excitation 325 nm), at 8.6 nM ANT-TTX. (D) The kinetics of AAG-TTX photolysis in the presence of axolemma. Axolemma were present at 3.27 mg/mL and AAG-TTX at a concentration of 0.027 μM. The increase in quantum yield of the reaction product as a function of time was monitored by measuring the increase in fluorescence at 415 nm (—) and in the presence of 10 μM TTX (-·-). At time = 0, high intensity 300-nm irradiation from the spectrofluorometer illuminated the sample by using 16-nm slit widths. (---) Fluorescence spectrum of the photolyzed product (excitation 345 nm) after illumination for 10 min.

NMAG-TTX (excitation 350 nm, emission 425 nm) is presented in Figure 6. Double-reciprocal plots of the data are linear, indicating a single class of sites with K_d = 8 nM. Fluorescence excitation scans (emission isolated with Schott KV 418 filter) reveal that, in addition to the 352-nm excitation peak, a 290-nm excitation peak also shows a similar enhancement as NMAG-TTX binds. Since NMAG-TTX does not have a significant absorption peak at 290 nm and the protein concentration was constant, this peak is apparently due to energy transferred from tryptophan residues to NMAG-TTX. At saturation, an energy transfer efficiency of 0.18 can be calculated from the enhancement of anthraniloyl fluorescence. The two peaks show parallel saturation, indicating that the TTX binding site causing fluorescence enhancement may be near one or more tryptophan residues.

For determination of whether the NMAG-TTX fluorescence enhancement is due to specific binding at the TTX receptor site, a similar experiment was performed by using membranes preequilibrated with 10 μM TTX. At high concentrations of fluorescent TTX, an equal concentration of TTX membranes showed only 20% as much fluorescence enhancement as nonpreequilibrated membranes and probably represents nonspecific binding. It is also possible, however, that during the time period required to make the measurement some TTX was displaced from the receptor site, resulting in the 20% increase in fluorescence observed. The formation of the fluorescent TTX–receptor complex is reversible, and the fluorescent reagent can eventually be displaced by TTX. When 10 μM TTX was added to membranes preincubated with 9 nM NMAG-TTX, a slow reduction in the emission at 425 nm was observed, and a first-order rate constant of 0.0097 s^{-1} was determined from a semilogarithmic plot of fluorescence intensity decrease vs. time. When a K_d of 3.2 × 10^{-9} M is used, the association rate constant can be estimated to be 3.0 × 10^{+6} M^{-1} s^{-1}, considerably slower than the diffusion-controlled limit.

The changes in the fluorescence anisotropy of the TTX derivatives were also used to follow the association of the ligand with the receptor site. With excitation at 350 nm, the limiting

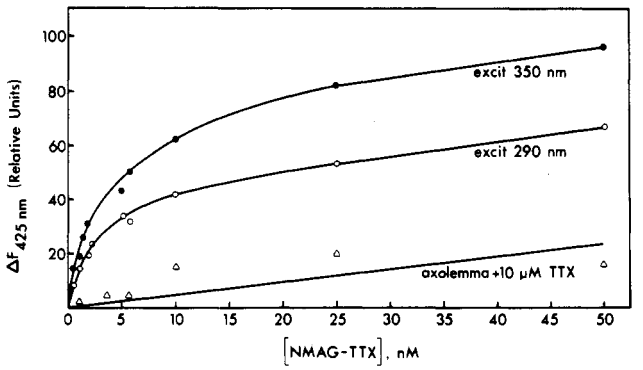

FIGURE 6: Fluorescence enhancement of NMAG-TTX upon binding to axolemma. Excitation was at 350 nm in the presence of 10 μM TTX (△) or absence of TTX (●) or at 290 nm (○), and emission was at 425 nm. The fluorescence of free NMAG-TTX was subtracted away. All three titrations had 1.35 mg of axolemma and identical instrument settings.

fluorescence emission anisotropy (anisotropy in the absence of macromolecular rotation) at 425 nm was determined to be 0.332 for NMAG-TTX. The equilibrium binding of NMAG-TTX and ANT-TTX to axonal membranes was studied by titrating a fixed concentration of membrane protein with increasing amounts of NMAG-TTX or ANT-TTX and measuring the resultant equilibrium fluorescence anisotropy values. The anisotropy as a function of total NMAG-TTX concentration is shown in Figure 7. Equation 4 relates the bound (L_B) to free (L_F) ratio of NMAG-TTX to the observed fluorescence anisotropy, r

$$L_B/L_F = (Q_F/Q_B)\frac{r - r_F}{r_B - r} \quad (4)$$

where Q is the fluorescence quantum yield. Measurements of anisotropy values of NMAG-TTX in the absence of membranes gave $r_F = 0.025$. r_B was determined to be 0.241 by extrapolation of anisotropy data obtained with different amounts of membrane protein as according to Levison (1975). The Q_F/Q_B ratio was determined to be 0.21. Scatchard analysis of these data for NMAG-TTX (inset, Figure 7) reveals one class of binding sites with a dissociation constant of 8.3 nM, in good agreement with the equilibrium parameters which were determined by either the direct displacement method or the fluorescence enhancement method. The data are summarized in Table I. When 10 μM TTX was added, a time-dependent decrease in the fluorescence anisotropy could be measured, with a half-life for the process of approximately 3 min. The anisotropy value of 0.241 reveals that the associated fluorescent toxin has limited rotational mobility and assumes a somewhat rigid and tight association with the receptor binding site.

Fluorescence Photoaffinity Labeling. The absorption maximum of AAG-TTX is 254 nm, and the presence of the axido group quenches the fluorescence due to a low-energy n–π* transition. Upon illumination, the spectral properties dramatically change, and there is a large increase in the fluorescence quantum yield as the nitrene generated reacts to produce substituted amines at the 2 position of the aromatic ring (Figure 5D). This feature has enabled the kinetics of the photolytic reaction to be monitored. The first-order rate constant for photolysis and fluorescence enhancement is 0.0048 s^{-1} with irradiation at 300 nm and can be increased by irradiating the sample at the absorbance maximum of 254 nm where the extinction coefficient is significantly higher. In addition, the rate of photolysis may be varied by altering the lamp intensity or thickness of the membrane suspension.

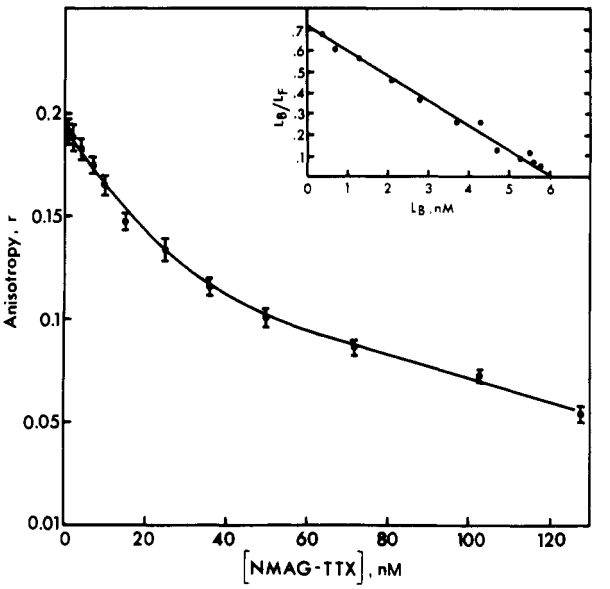

FIGURE 7: Titration of NMAG-TTX binding to axonal membranes by changes in fluorescence emission anisotropy. A fixed amount of axonal membranes (1.56 mg/mL) was titrated with increasing amounts of NMAG-TTX at 25 °C. Excitation was at 350 nm, and the fluorescence in both emission channels was isolated with Schott KV 418 filters. The data presented represent the mean of five determinations. (Inset) Scatchard analysis of these data plotted according to eq 4.

Photolysis in the presence of 10 μM TTX showed that approximately 15% of the fluorescence intensity centered about 415 nm is due to nonspecific labeling under these experimental conditions.

Fluorescence anisotropy measurements with membranes incubated with AAG-TTX, photolyzed, and washed free of unreacted AAG-TTX indicated a more rigid orientation of the probe (anisotropy = 0.290), as would be expected for a covalently inserted moiety. Addition of 10 μM TTX did not change either the fluorescence intensity or the fluorescence anisotropy properties of the photolyzed AAG-TTX bound to the membranes.

Discussion

Because of the relatively low concentration of sodium channels compared with other membrane components in excitable membranes, the isolation and characterization of these proteins are made very difficult. Certain aspects of the molecular structure and mechanism of action of the Na^+ channel in intact excitable membranes, however, can be determined by introducing spectroscopic probes into specific functional sites on the macromolecule.

It has been suggested that the sodium channel is composed of distinct molecular structures which are represented by the "ion selection center", the "activation gate", and the "inactivation gate". Tetrodotoxin is very useful for identifying Na^+ channels since it eliminates the inward sodium current and not the sodium gating current (Hille, 1970, 1975b, 1978). Only external application of the toxin is effective (Narahashi et al., 1967). On the basis of a number of such observations, a model has been proposed whereupon TTX binds tightly to the "ion-selectivity filter" of the channel, thereby blocking the entry of sodium ions (Hille, 1978). By incorporation of a fluorophoric moiety into TTX, the emission characteristics could be used to determine a number of static and dynamic features of this ion channel site which include the polarity, rigidity, dipolar relaxation, and the location of the TTX receptor relative to the activation and inactivation gates by

Förster fluorescence energy transfer.

Our first attempts were directed toward esterification of [7-(dimethylamino)coumarinyl]aminopropionic acid to the primary C_{11} hydroxyl of TTX by the carbodiimidazole method. Previous reports suggested that the biological activity of TTX is retained after derivatization at this site by this method (Guillory et al., 1977). Although the esterification reaction appeared successful, numerous difficulties were encountered. Thin-layer chromatographic analysis revealed many reaction products as well as significant amounts of unreacted or hydrolyzed toxin which were difficult to separate and purify. Furthermore, slow hydrolysis of the ester derivative upon storage precluded the use of this method.

Rather, our efforts turned toward converting the C_6 and C_{11} hydroxyls of TTX to a ketone at position 6 to synthesize fluorescent hydrazone derivatives. The ketone could also be reductively aminated to 6-amino- or 6-(methylamino)-TTX for the preparation of amide derivatives of TTX. In particular, acylation of NH_2-TTX by the *N*-succinimidyl ester of mono[^{125}I]iodo(hydroxyphenyl)propionic acid has enabled us to prepare a biologically active ^{125}I-iodinated derivative of TTX with a specific radioactivity of ~2000 Ci/mmol (N. W. Ross and K. J. Angelides, unpublished results; Angelides, 1980). This derivative is suitable for binding studies and is currently being used to determine the location and distribution of Na^+ channels in myelinated, unmyelinated, and experimentally demyelinated nerve fibers by light and electron microscope autoradiographic techniques. Previous work has clearly shown that position 6 in TTX can be used for chemical modifications without loss of biological activity of the toxin (Tsien et al., 1975; Chicheportiche et al., 1979, 1980). The first report using this modification described the preparation and mode of action of a photoaffinity reagent (Chicheportiche et al., 1979). The synthetic methods used in that work only led to yields which were on the order of 5–10% due in part to the low solubility of TTX in dimethylformamide, the angular nature of the ketone group, the hydrolysis of the hydrazone formed, and the apparent resistance to reduction by sodium cyanoborohydride. When the coupling reactions are carried out in slightly acidified organic solvents and, in particular, in the presence of molecular sieves, the yield of tetrodotoxin derivatives can be considerably improved. More recently the preparation of radiolabeled ^{3}H Schiff-base derivatives of TTX has been described (Chicheportiche et al., 1980).

Modification of the native toxin by introduction of a small aromatic residue has been shown to significantly perturb neither the biological activity nor the affinity for TTX to the sodium channel. The derivative which shows the lowest affinity for the sodium channel is AAG-TTX which forms a complex with its receptor about 5 times less tightly than the complex with native TTX. This is probably due to the size (~4 Å) and limited rotational freedom of the azido group. The *N*-methyl derivative, which is comparable in size to the azido group, binds about 2 times tighter than AAG-TTX and reflects the greater conformational mobility of the *N*-methyl group relative to the azido group.

The fluorescent derivatives of TTX reported here were synthesized in order to obtain information on the microenvironment about the "selectivity filter" of the sodium channel, to be used as donors in singlet–singlet fluorescence energy transfer, and to facilitate microscopic visualization of the channel in selected nerve fibers. The strategy was to employ fluorescent and photoactivatable fluorescent reagents that could be attached to TTX, would bind tightly to the designated site on the ion channel, and would satisfy the desired spectroscopic requirements. In addition, the spectroscopic reagents were designed that, while still retaining selective and high affinity of binding for the site to be studied, would contain a reactive (or activatable) functional group and a profluorophore that could serve as a sensitive marker for the labeling of the target macromolecule.

Derivatives of anthranilic acid fulfill many of these requirements and have several distinct advantages: (1) They are probably the smallest fluorescent reagents available and ones that would least modify either the biological activity or the binding properties of the native toxin. (2) Their chemistry allows coupling to either carboxyl or amino groups as well as possibilities to transform the 2-amino to other functional groups. (3) The spectroscopic properties are such that they can act energy acceptors from tryptophan fluorescence and can serve as fluorescent energy donors to a large array of energy acceptors. (4) Anthraniloyl compounds are very environmentally sensitive, have efficient quantum yields, and exhibit excited-state lifetimes which can be conveniently measured by either phase-modulation or pulse-sampling techniques. Although the quantum yields of anthranilic acid derivatives are high (~0.6), the compounds have the one disadvantage in that the extinction coefficients are generally relatively low (4000–6000 M^{-1} cm^{-1}).

When the TTX derivatives bind to axolemma, marked changes in the fluorescence emission intensity and maxima are observed. There are three possible explanations for this fluorescence enhancement upon binding to axonal membranes: (1) the enhancement arises from the displacement of water at the receptor site; (2) the fluorescent derivatives of TTX are quenched in polar solvents due to excited-state proton transfer; (3) the anthraniloyl chromophore is quenched by a charge-transfer interaction with the guanidinium group of TTX.

Because the fluorescence emission intensity of free NMAG increases as the polarity of the solvent increases (Table II), it is unlikely that water displacement can account for the fluorescence increase. So that the second possibility could be tested, the fluorescence yield and emission maxima of NMAG and ANT were measured as a function pH. They are invariant over the pH range from 2.5 to 12.0. But below 2.5, the fluorescence decreases as the 350-nm absorbance decreases, reflecting ground-state protonation. Furthermore, addition of D_2O showed a higher fluorescence intensity than addition of H_2O. However, the ethyl ester of dimethylanthranilic acid, which has no ionizable proton, shows similar enhancement as in D_2O. Thus it seems unlikely that excited-state proton transfer is responsible for the observed quenching of NMAG-TTX fluorescence in aqueous solution. The third possibility was examined by constructing CPK molecular models. NMAG-TTX may assume a folded conformation where the fluorescent aromatic ring forms a charge-transfer complex with the guanidinium group of the toxin. Upon binding of NMAG-TTX to axonal membranes, the charged guanidinium group inserts into the channel, resulting in a more extended conformation of the toxin, and thereby gives rise to the fluorescence enhancement.

The excitation and emission maxima of the anthraniloyl derivatives vary with solvent polarity so that the immediate environmental characteristics of the TTX receptor can be inferred. The emission maximum of the NMAG-TTX receptor complex is 439 nm while NMAG emits at 432 nm in water and 406 nm in dioxane. The other compounds show the same red shift in the emission maximum with increasing solvent polarity, an effect generally observed for fluorescent molecules that possess a substantial dipole moment in the

excited state (Haugland & Stryer, 1967; Weber & Farris, 1979). The spectral broadening data also provide independent confirmation that the environment of the anthraniloyl group is highly polar (Marcus, 1965; Weber & Farris, 1979). The 7-nm red shift observed from water bound to the receptor could arise from a fixed element at the receptor site which is highly polarized and opposes the stabilized excited state, from solvent reorientation, or from rapid reorientation of some polar structure at the receptor site. The latter points have been examined by increasing the viscosity of the medium such that no appreciable solvent rearrangement is possible over the excited-state fluorescence lifetime. At −40 °C and in 50% ethylene glycol, a 30-nm blue shift is observed in both the free fluorophore and fluorophore + membrane emission spectra, suggesting that the observed red shift is due, at least in part, to enhanced solvent relaxation. More information on the dipolar relaxation characteristics of the probe in this environment and the capacity of this environment to reorient itself during the excited state can be obtained by measuring the fluorescence lifetime across the emission band under more physiological conditions.

It has been suggested that the toxin binding site is composed of hydrophilic protein groups which serve both to bind the toxin and to dehydrate the sodium ion as one of the initial events in the passage of sodium ions through the channel (Hille, 1978). Chemical modification and electrophysiological measurements have shed some light on the molecular character of the ion channel. Inhibition of TTX binding by modification with tetramethyloxonium tetrafluoroborate has demonstrated the importance of a carboxylate for binding of toxin to the receptor (Reed & Raftery, 1976). Electrophysiological measurements in the presence of D_2O suggest that formation of conducting channels involves large changes in local solvent structure (Schauf & Bullock, 1979). The spectral data lend further support to the idea that the "selectivity filter" at the Na^+ channel is highly polar and that binding of TTX reorients solvent molecules or some polar element at the toxin receptor site.

The fluorescence anisotropy data indicate that the anthraniloyl group at the toxin receptor site has restricted conformational mobility and probably reflects the limited conformational states that the receptor site can assume. It is now possible to investigate conformational transitions of the macromolecular site by using the fluorescence emission or polarization characteristics of anthraniloyl-TTX upon binding of other channel ligands (e.g., scorpion toxins, veratridine, and batrachotoxin), by changing the transmembrane potential, or by alterating the interaction with the membrane.

Electronic energy is transferred from a tryptophan residue to the anthraniloyl group and is demonstrated by the sensitized fluorescence of the anthraniloyl group bound at the channel receptor site. By use of a R_0 of 20 Å (with the assumption that $K^2 = {}^2/_3$ and that the chromophores are randomly oriented with respect to each other) for tryptophan to anthraniloyl transfer (Haugland & Stryer, 1967), a distance of approximately 26 Å for a single donor–acceptor pair can be calculated. Since the number of tryptophans is unknown, it is not possible to determine a precise distance between the donor and acceptor groups, although by more detailed studies and by the application of appropriate models, constraints on the location of these groups can be determined (Fung & Stryer, 1978; Baird et al., 1979; Angelides & Hammes, 1979; Dewey & Hammes, 1980).

This report also describes the synthesis, mode of action, and spectral properties of a photoactivatable fluorescent TTX derivative. Photoactivatable fluorescent active site directed azidoanthraniloyl probes have been synthesized and used for detailed kinetic, photolabeling, and spectral studies with the serine proteases, α-chymotrypsin, and trypsin (Angelides, 1981). From the results of these studies, useful spectroscopic derivatives of TTX could be tested. The data suggest that AAG-TTX is a true and highly specific photoaffinity label that requires light irradiation for covalent bonding and concomitant fluorescence to take place at the toxin receptor site. The fluorescence signal of the specifically bound label is sufficiently strong and also indicates that the binding site is composed of a highly polar and immobilized environment. By use of the fluorescent photoaffinity label, specific attachment of an extrinsic fluorescent probe to the desired ion channel site in a complex mixture of membrane proteins or a macromolecular assembly has been accomplished. One has both a marker for the covalent bond insertion, the nature of the chemical bond, and the placement of spectroscopic label at a carefully chosen locus. The observed fluorescence of such labeled proteins is more amendable to interpretation due to a better knowledge of the location of the reporter group within the studied assembly. It can also provide a sensitive handle toward isolation and purification of the ion channel.

The application of photoactivatable fluorescent reagents has been extended toward cleavable photoactivatable fluorescent probes (azo- or *vic*-glycol linkages). Preliminary experiments with cleavable analogues of azidoanthraniloyl-TTX show that, after irradiation, application of small amounts of periodate, followed by washing, removes the TTX moiety and leaves the fluorescent tag attached. Thus it may be possible to prepare a functional channel with a fluorescent reporter group at or near the "selectivity filter".

It is hoped that these reagents will provide useful TTX derivatives to obtain molecular details on the structure and mechanism of action of the sodium channel in excitable membranes. A number of spectroscopic glyoxal derivatives have recently been prepared to label an arginine residue which has been implicated as forming part of the gating structure (Rojas & Rudy, 1976; Eaton et al., 1978; Nonner et al., 1980). These derivatives are currently being utilized to map out the functional sites of the sodium channel by fluorescence resonance energy transfer measurements.

Acknowledgments

I thank Neil Ross for preparation of axonal membranes, Dr. Richard P. Haugland, Molecular Probes, for very helpful discussions, and Dr. A. L. Padjen, Department of Pharmacology, McGill University, for the electrophysiological measurements. I am also grateful to B. Soowamber for the preparation of this manuscript and extraordinary patience.

References

Agnew, W. S., & Raftery, M. A. (1979) *Biochemistry 18*, 1912–1919.

Agnew, W. S., Levinson, S. R., Brabson, J. S., & Raftery, M. A. (1978) *Proc. Natl. Acad. Sci. U.S.A. 75*, 2606–2610.

Angelides, K. J. (1980) *Neurosci. Meet. Abstr.*, 108.5.

Angelides, K. J. (1981) *Biochim. Biophys. Acta* (in press).

Angelides, K. J., & Hammes, G. G. (1979) *Biochemistry 18*, 1223–1229.

Armstrong, C. M. (1975) *Q. Rev. Biophys. 7*, 179–210.

Azumi, T., & McGlynn, S. P. (1962) *J. Chem. Phys. 37*, 2413.

Baird, B., Pick, U., & Hammes, G. G. (1979) *J. Biol. Chem. 254*, 3818–3825.

Balerna, M., Fosset, M., Chicheportiche, R., Romey, G., & Lazdunski, M. (1975) *Biochemistry 14*, 5500–5511.

Benzer, T. I., & Raftery, M. A. (1972) *Proc. Natl. Acad. Sci. U.S.A. 69*, 3631–3637.
Bradford, M. J. (1976) *Anal. Biochem. 72*, 248–254.
Cantley, L. C., & Hammes, G. G. (1973) *Biochemistry 12*, 4900–4904.
Chicheportiche, R., Balerna, M., Lombet, A., Romey, G., & Lazdunski, M. (1979) *J. Biol. Chem. 254*, 1552–1557.
Chicheportiche, R., Balerna, M., Lombet, A., Romey, G., & Lazdunski, M. (1980) *Eur. J. Biochem. 104*, 617–623.
Cohen, S. R., McKhann, G. M., & Guarnieri, M. (1975) *J. Neurochem. 25*, 371–376.
Dale, R. F., & Eisinger, J. (1975) *Biochem. Fluoresc. Concepts 1*, 115.
De Vries, G. H., Mathieu, J.-M., Beny, M., Chicheportiche, R., Lazdunski, M., & Dolivo, M. (1978) *Brain Res. 147*, 339–352.
Dewey, G. W., & Hammes, G. G. (1980) *Biophys. J. 32*, 1023–1036.
Eaton, D. C., Brodwick, M. S., Oxford, G. S., & Rudy, B. (1978) *Nature (London) 271*, 473–476.
Fung, B. K.-K., & Stryer, L. (1978) *Biochemistry 17*, 5241–5248.
Guillory, R. J., Rayner, M. D., & D'Arrigo, J. S. (1977) *Science (Washington, D.C.) 196*, 883–885.
Haugland, R. P., & Stryer, L. (1967) *Conform. Biopolym., Papers Int. Symp. 1*, 321–335.
Henderson, R., & Wang, J. H. (1972) *Biochemistry 11*, 4565–4569.
Hille, B. (1970) *Prog. Biophys. Mol. Biol. 21*, 1–32.
Hille, B. (1975a) *Biophys. J. 15*, 615–619.
Hille, B. (1975b) *Membranes 3*, 255.
Hille, B. (1978) *Biophys. J. 22*, 283–295.
Holowka, D. A., & Hammes, G. G. (1977) *Biochemistry 16*, 5538–5545.
Levison, S. (1975) *Biochem. Fluoresc. Concepts 1*, 375.
Marcus, R. A. (1965) *J. Chem. Phys. 43*, 1261–1268.
Mosher, H. S., Fuhrman, F. A., Buchwald, H. O., & Fischer, H. G. (1964) *Science (Washington, D.C.) 144*, 1100–1110.
Narahashi, T., Moore, J. W., & Poston, R. N. (1967) *Science (Washington, D.C.) 156*, 976–979.
Nonner, W., Spalding, B. C., & Hille, B. (1980) *Nature (London) 284*, 360–363.
Nũnez, M. T., Fischer, S., & Jaimovich, E. (1976) *Anal. Biochem. 72*, 320–325.
Parker, C. A., & Rees, W. T. (1966) *Analyst (London) 85*, 587–594.
Reed, J. K., & Raftery, M. A. (1976) *Biochemistry 15*, 944–953.
Ritchie, J. M., & Rogart, R. B. (1977) *Rev. Physiol., Biochem. Pharmacol. 79*, 1–20.
Rojas, E., & Rudy, B. (1976) *J. Physiol. 262*, 501–531.
Ross, N. W., & Angelides, K. J. (1980) *Pap. Meet.—Am. Chem. Soc., Div. Biol. Chem.*, 96.
Schauf, C. F., & Bullock, J. O. (1979) *Biophys. J. 27*, 193–208.
Scott, T. G., Spencer, R. D., Leonard, N. J., & Weber, G. (1970) *J. Am. Chem. Soc. 92*, 687–692.
Shinitzky, M. (1972) *J. Chem. Phys. 56*, 5979–5984.
Staiger, R. P., & Miller, E. B. (1959) *J. Org. Chem. 24*, 1214–1222.
Strong, P. N., & Keana, J. F. W. (1976) *Bioorg. Chem. 5*, 255–262.
Strong, P. N., Smith, J. T., & Keana, J. F. W. (1973) *Toxicon 11*, 433–438.
Tsien, R. Y., Green, D. P. L., Levinson, S. R., Rudy, B., & Sanders, J. K. M. (1975) *Proc. R. Soc. London, Ser. B 191*, 555–559.
Varlet, J.-M., Collignon, N., & Savignac, P. (1978) *Synth. Commun. 8*, 335–343.
Velapoldi, R. A., & Mielenz, K. D. (1980) *NBS Spec. Publ. (U.S.)*, 260–264.
Weber, G., & Farris, F. J. (1979) *Biochemistry 18*, 3075–3078.